Hindawi Publishing Corporation
Advances in Condensed Matter Physics
Volume 2010, Article ID 518209, 6 pages
doi:10.1155/2010/518209

Research Article

Electrical Characteristics and Nanocrystalline Formation of Sprayed Iridium Oxide Thin Films

S. A. Mahmoud,[1,2] S. M. Al-Shomar,[1] and A. A. Akl[2]

[1] *Physics Department, Faculty of Science, Hail University, Hail, Saudi Arabia*
[2] *Physics Department, Faculty of Science, El-Minia University, El-Minia 11511, Egypt*

Correspondence should be addressed to S. A. Mahmoud, samahmoud2002@yahoo.com

Received 27 July 2009; Accepted 29 March 2010

Academic Editor: Ward Beyermann

Nanostructure and electrical properties of iridium oxide (IrO_2) thin films prepared by spray pyrolysis technique (SPT) have been experimentally characterized. The effect of solution molarity (SM) and substrate temperature (T_{sub}) on the nanostructure features and electrical conductivity of these films has been investigated. The results of X-ray diffraction (XRD) showed that all samples prepared at $T_{sub} = 350^{\circ}C$ with different SM, IrO_2 appear almost in amorphous form. XRD revealed that the films deposited at $T_{sub} = 450^{\circ}C$ were tetragonal structures with a preferential orientation along ⟨101⟩ direction. Moreover, the degree of crystallinity was improved by solution molarity. Single order Voigt profile method has been used to determine the nanostructure parameters at different SM and T_{sub}. The dark conductivity measurements at room temperature as a function of SM were observed and the value of conductivity were slightly increases at higher SM, reaching the bulk value of 20 $\Omega^{-1}cm^{-1}$. The values of activation energy of ΔE and σ_o of IrO_2 were found to be 0.21 eV and $1.68 \times 10^{-3}\Omega^{-1} \cdot cm^{-1}$, respectively.

1. Introduction

Among the transition metal oxide, iridium oxide has attracted considerable interest over the years owing to its wide range of applications. The interest of iridium oxide has been growing due to its remarkable chemical, electrochemical, and physical properties, including pH-sensing [1, 2], chlorine, ammonia, or oxygen evaluation [3], neural stimulation [4], field emission cathode [5], advanced memory technology [6], and electrochromic devices and optical information storage [7]. Furthermore, it is used as coating for electrodes in functional electrical stimulation [8]. The electrodes are used to electrically excite nerve cells. The application draws on biocompatibility, high electrochemical activity, and corrosion resistance. The technology of the electrochromic thin films becomes more and more attractive for researchers. The interest for electrochromic materials is based on their potential applications to smart windows, gas sensors and high contrast nonemissive information display system, and devices for thermal control [9]. IrO_2 thin film is one of the most promising electrochromic electrodes. One of the advantages of iridium oxide film is the influence of doping on the crystallite size and hence the coloration efficiency [10]. The disadvantage of Ir-oxide layer is its small coloration efficiency (CE) which is about 11 cm^2/C in comparison to that of tungsten oxide, CE = 37 − 50 cm^2/C [11].

Several more adequate deposition techniques were employed for synthesis of thin films of Ir-oxide such as sputtering [12], liquid delivery metal-organic (MOCD) [13], sol-gel process [14], pulsed laser deposition [15], thermal evaporation process [16], and spray pyrolysis [17]. Most of these techniques are either not feasible or too expensive for industrial applications. The spray pyrolysis process is an attractive low-cost, versatile method for synthesis of thin films. Furthermore, this method has been used intensively lately for the preparation of different types of thin film, especially of oxides and sulfides of many metals and semiconductors [18, 19]. The advantage of spray pyrolysis is manifold; microstructure of the film can be altered depending on the spray condition, repeatability, adherent deposition, and easy doping.

The aims of the present study are as follows:

(i) to investigate the effect of the T_{sub} and SM on the synthesis of a single phase of IrO_2 thin films were deposited by using spray pyrolysis iridium chloride ($IrCl_3 . 3H_2O$) as starting solution onto heated glass substrate.

(ii) to investigate and discuses the influence of the T_{sub} and SM on the crystalline growth of nanostructure and electrical properties of the obtained samples were studied in order to determine the suitable temperature and molarity to produce a single phase of IrO_2.

2. Experimental Details

Thin films of Ir-oxide were deposited by spray pyrolysis technique (SPT) from aqueous solution of iridium chloride ($IrCl_3 . 3H_2O$) onto preheated glass substrate at two temperatures 350 and 450°C. The solution at different concentrations (0.005–0.03 M) was sprayed through glass nozzle using air as a carrier gas onto the ultrasonically cleaned substrate. The overall reaction process was expressed as thermal decomposition of iridium chloride to form clusters of Ir-oxide, in the presence of the water, as follows:

$$2IrCl_3 + 3H_2O \longrightarrow Ir_2O_3 + \quad 6HCl \uparrow . \tag{1}$$

The heat annealed process at 600°C for 120 minutes was made of all prepared samples at different SM and T_{sub}. The chemical reaction that took place was as follows:

$$Ir_2O_3 + \frac{1}{2}O_2 \xrightarrow{600^\circ C, 120\,\text{minutes}} 2IrO_2. \tag{2}$$

The resulting films were found to be uniform, strongly adherent to the substrates, and blackish in colour. A controller of temperature was used to measure the T_{sub} using the resistance heater via a thermocouple. In order to get homogeneity thin films, the height of the spraying nozzle and the rate of the spray process were kept constant during the deposition process at 25 cm and 5 cm^3/min, respectively.

The structure characteristics of the films were studied using by X-ray diffractometer (JEOL model JSDX-60PA) with attached Ni-filtered Cu-K_α radiation (λ = 0.154184 nm). Continuous scanning was applied with a slow scanning speed (1°/min) and a small time constant (1 second). A range of two theta (from 25° to 70°) was scanned, to insure the detection of all possible diffraction peaks detected. Nanostructure and the phase identification of the polycrystalline thin film of IrO_2 at different SM and T_{sub} were investigated. The crystallite size and macrostrain of the films were determined using single order Voigt profile analysis [20]. The average values of FWHM of the characterized peaks were measured after correction of instrumental factor. Numerical calculation was developed using the refractive indices of crystalline, amorphous, and single crystal of IrO_2 as in (6) to estimate the crystalline volume fraction. Also, the film thicknesses of the prepared samples were measured using mechanical stylus method (MSM) (Sloan Dektak, model 11A) [21].

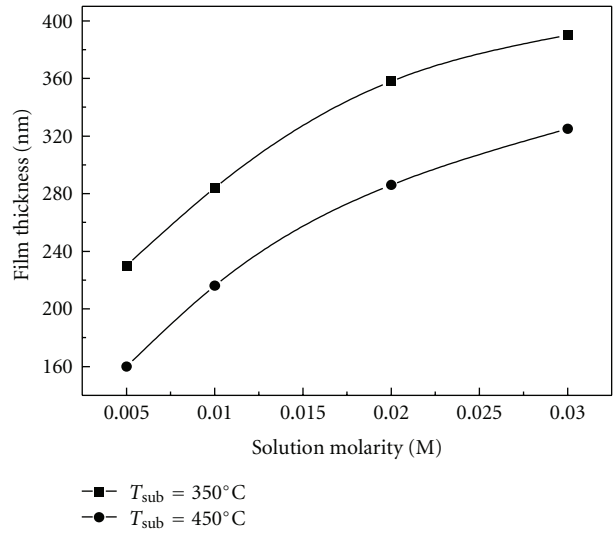

Figure 1: The thickness of IrO_2 films versus solution molarity prepared at substrate temperatures 350°C and 450°C.

The DC of electrical conductivity measurement was performed on the films using by four-point probe technique of Van der Pauw [22] at room temperature with the required correction tables [23]. Two gold electrodes were deposited on the iridium oxide/glass samples leaving an uncoated trip in the middle. A constant-load spring was used for the contact. The current-voltage characteristics were measured using Keithely digital electrometer (Model 616).

3. Results and Discussion

3.1. Film Thickness Measurements. Ir-oxide film thicknesses prepared at two substrate temperatures (350 and 450°C) with different SM and constant deposition time (DT) of 10 minutes were measured by MSM. Figure 1 shows the variation of the film thickness of IrO_2 as a function of solution molarity (SM). It is clear that, the film thicknesses of the prepared samples at T_{sub} = 350°C have a higher value than those at another temperature. This is because the evaporation rate was increased at higher temperature, leading to diminished mass transport outwards the substrates, which is a decrease of film thickness. Furthermore, at rise of the solution molarity, the values of film thickness increased. Each data point is the average of five measurements taken at different locations on the film surface; the calculated error was found to be ±5%. Consequently, these results may suggest that the different temperature and SM of sprayed films have a significant influence on the film thickness of the IrO_2 films. Similar results were previously described using NiO_2 film on glass substrate [18].

3.2. Formation of Single Phase Ir-Oxide. Figure 2 depicts the variation of the diffraction patterns as a function of SM while the T_{sub} of 350°C and DT of 10 minutes were kept

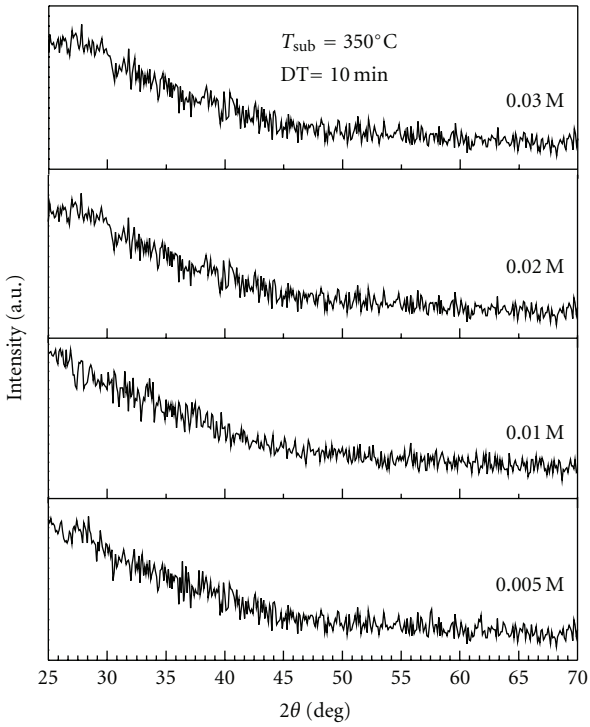

Figure 2: X-ray diffraction patterns for IrO_2 films as a function of solution molarity at T_{sub} = 350°C and deposition time = 10 minutes.

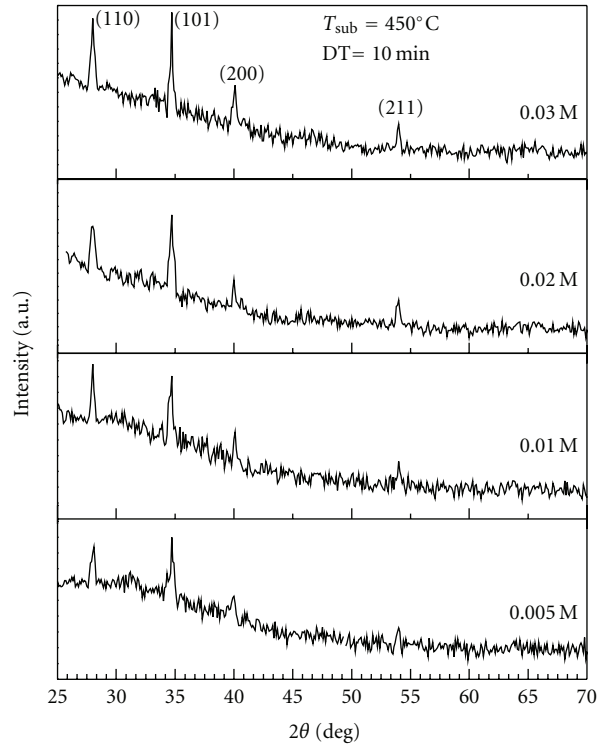

Figure 3: X-ray diffraction patterns for IrO_2 films as a function of solution molarity at T_{sub} = 450°C and deposition time = 10 minutes.

constant. The results of XRD for all samples as-deposited at T_{sub} = 350°C show that the film structure was noncrystalline phase with different SM, while at T_{sub} = 450°C, the films were fully transformed to polycrystalline phase of IrO_2 which had a tetragonal structure when SM varies (Figure 3). The presence of the characteristic lines corresponding to (110), (101), (200), and (211) planes of IrO_2 was observed which coincide with ICDD number 15–870. The increase in the amount and the crystallinity of the phase were exhibited at raising the SM which is indicated by the enhancement of intensity and decrease of FWHM in peaks. Also, the increase in the intensity of the peaks may be attributed to either grain growth associated with smallest thickness or the increase in the degree of crystallinity by increasing the temperature or both.

The average values of calculated lattice parameters were found to be a = b = 4.498 Å and c = 3.154 Å which coincide with the bulk of IrO_2 [24]. Moreover, the films show preferred growth along direction < 110 > and < 101 > as SM increases. Also, no other additional peaks corresponding to other phases have emerged. This suggests that IrO_2 phase is stable and its formation is independent of SM.

3.3. Nanostructure Characteristics of IrO_2 Films. The IrO_2 thin films were analyzed by XRD technique to study nanostructural parameters (crystallite/domain size and macrostrain) under several SM and temperatures. The crystallite/domain size is by definition measured in the direction normal to the diffraction plane and consequently perpendicular to the substrate. Therefore, the observed increase in the crystallite/domain size may be interpreted in terms of a columnar grain growth. The macrostrain is equivalent to a variation in interplanar spacing within domains by amount which depends on the elastic constants of the material and the nature of internal stresses. Viogt method for single-order profile analysis was used to calculate the crystallite/domain size and macrostrain of the polycrystalline IrO_2 films [25]. The parameter of interest with the Voigt function is "the shape parameter" which is defined as [w = FWHM/integral breadth]. The value of the shape parameter, ranging from 0.6366 to 0.9395, was used to determine the fractional Lorentzian (Chuchy) β_{fl} and Gaussian β_{fG} components in the convolute. The Lorentzian (Chuchy) and Gaussian components of the integral breadth of pure specimen profile are given by

$$\beta_{fl} = \beta_{hl} - \beta_{gl},$$
$$(\beta_{fG})^2 = (\beta_{hG})^2 - \left(\beta_{gG}\right)^2, \tag{3}$$

where h, f, and g are the observed, specimen, and instrumental profile function, respectively. The apparent crystallite/domain size ε is

$$\varepsilon = (\beta_{fl})^{-1} \text{ (Lorentzian)}, \quad \varepsilon = (\beta_{fG})^{-1/2} \text{ (Gaussian)}. \tag{4}$$

The calculated average crystallite/domain size according to the four diffraction planes (110), (101), (200), and (211)

at different SM using by Lorentzian as well as Gaussian component is given in Table 1. It is clear that the value of crystallite size is slightly increased at different SM. This means that the variation in crystallite size was observed due to the mobility and concentration of ions which is appropriate for crystal growing on the substrate. Kawar et al. reported the same value of grain size for the like phase prepared by spray pyrolysis [26].

The macrostrain $|e|$ of investigated samples was determined using Voigt method formula:

$$|e| = \frac{\Delta d}{d_o} = \frac{1}{2}\cot\theta \cdot \Delta\theta, \tag{5}$$

Where d_o is the standard value of interplanar spacing taken from JCPDS data file [17-870]. The macrostrain was calculated as an average of fractional change, $\Delta d/d_o$, in the interplanar spacing, d, of the four diffraction planes (110), (101), (200), and (211). The calculated macrostrain for all prepared samples at different SM is given in Table 1. It is clear that the macrostrain was decreased as a function of SM, which indicates that the sprayed molecules are ejected with higher kinetic energy and momentum. Therefore, these molecules recombine with higher mobility energy causing variations to occur within their internal stress and consequent macrostrain decrement.

3.4. Crystalline Volume Fraction. The crystalline volume fraction of IrO_2 thin film as a function of SM was estimated by the analysis of the optical reflectivity spectra in the ultraviolet region [27, 28]. The crystalline volume fraction, X_C, is defined by the following equation:

$$X_C = \left(\frac{n_C - n_A}{n_S - n_A}\right), \tag{6}$$

where n_C, n_A, and n_S are the complex refractive indices for nanocrystalline, amorphous, and single crystalline IrO_2, respectively. The volume fraction of the crystalline IrO_2 was obtained by fitting the calculated reflectivity spectra to experimental reflectivity spectra. The crystalline volume fraction, X_C, was estimated for nanocrystalline IrO_2 films at different SM listed in Table 2. It can be observed that the increase in the SM induces a change in the amorphous-crystalline transition, showing an increase in X_C in the investigated samples. This fact is related to a crystallization of the material for higher substrate temperature and SM [29].

3.5. Dark Electrical Conductivity of IrO_2 Films. To measure the electrical conductivity, two ways of investigation were done, one of them at room temperature and the other at different temperature. The values of DC electrical conductivity as a function of solution molarity of IrO2 films prepared at 350 and 450°C were measured at room temperature, using four-point probe technique shown in Figure 4. It was found that the values of electrical conductivity of amorphous are lower than nanocrystalline structure, and it increases rapidly with increasing SM for both substrate temperatures. This is because the film thickness increases as concentration increases. Thus the increase in crystallite size resulted in

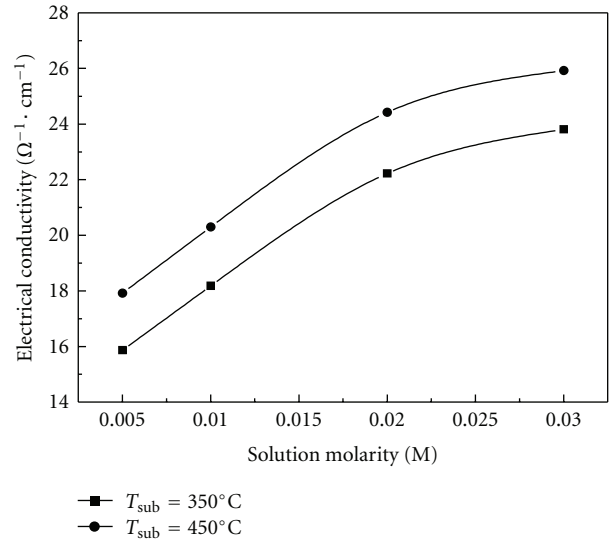

Figure 4: The dark electrical conductivity of IrO_2 thin film as a function of solution molarity at different substrate temperatures.

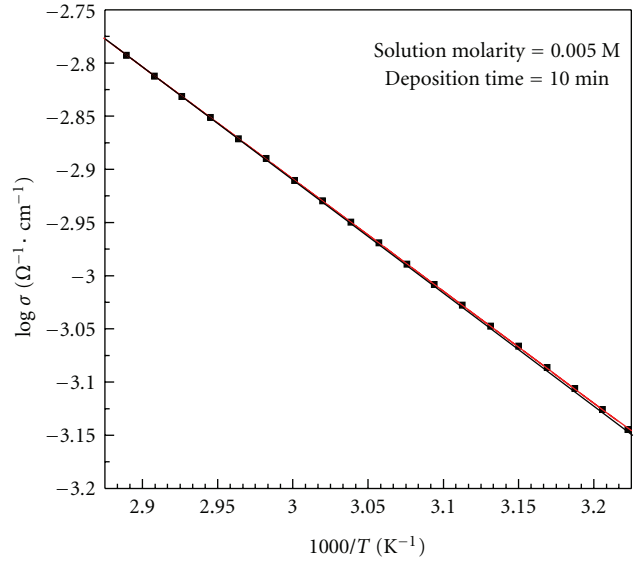

Figure 5: Plots of Log σ versus 1000/T for IrO_2 thin film.

the reduction of grain boundary associated with electrons scattering and thence increase in electrical conductivity. Accordingly, the increment of electrical conductivity was correlated with the film morphology change of IrO2 film. Similar results have been previously reported [15, 30]. Also, the value of conductivity was found to be from 15.9 to 23.8 $\Omega^{-1}\cdot$ cm^{-1} when SM varies from 0.005 to 0.03 M, respectively.

3.6. Effect of Temperature on the Conductivity. At different temperature, the variation of conductivity against reciprocal absolute temperature was investigated. In iridium oxide, the dependence of conductivity on temperature is more complex because of different chemistry of decomposition. IrO_2 has

Table 1: The average crystallite size (nm) and macrostrain at different solution molarity (M) and kept constant substrate temperature of 450°C.

Solution molarity (M)	Lorentzian	Gaussian	Macrostrain ($\times 10^{-3}$)
0.005	11.56 ± 0.3	8.25 ± 0.2	1.96 ± 0.03
0.01	13.25 ± 0.3	9.03 ± 0.2	3.34 ± 0.03
0.02	15.38 ± 0.3	9.97 ± 0.2	3.18 ± 0.03
0.03	18.54 ± 0.3	10.38 ± 0.2	3.38 ± 0.03
Average value	14.68	9.41	2.97

Table 2: The crystalline volume fraction of IrO_2 thin films as a function of solution molarity.

Solution molarity (M)	n_A	n_C	n_S	X_C
0.005	2.54	2.65	2.16	0.289
0.01	2.68	2.86	2.16	0.346
0.02	2.88	3.18	2.16	0.417
0.03	2.96	3.35	2.16	0.487
Average value	2.765	3.010	2.16	0.385

been found to be nonstoichiometric with excess of oxygen [31]. The temperature dependence of electrical conductivity is given by the Arrhenius relation:

$$\sigma = \sigma_o \exp\left(\frac{-\Delta E}{KT}\right), \tag{7}$$

where σ_o is the pre-exponential factor, ΔE is the activation energy for DC conduction, K is the Boltzmann's constant, and T is the absolute temperature. The temperature dependent dc dark conductivity of IrO_2 thin films is shown in Figure 5. The plots of Log σ versus $1000/T$ were found to be straight line indicating that conduction is performed through an activated process having single activation energy in the temperature range from 303 to 350 K. This is attributed to the thermally assisted hopping of carriers between localized states closes to Fermi level [30]. The values of ΔE and σ_o were calculated from slope of the curve and were found to be 0.21 eV and $1.68 \times 10^{-3}\,\Omega^{-1} \cdot \text{cm}^{-1}$, respectively. The behavior of conductivity of these samples as a function of temperature was matched with sputtered iridium oxide thin film [25]. The various magnitude values of electrical conductivity that we found may indicate possible transformation of IrO_2 films from semiconducting phase to metallic one. This transition is conceived to be due to the change in oxidation state of iridium [31, 32], as a result of which the Fermi energy level, E_f, crosses the conduction band edge E_c.

4. Conclusions

Ir-oxide films have been prepared onto heated glass substrates from iridium chloride solution using SPT at different solution molarity and two substrate temperatures. As revealed by XRD, at $T_{\text{sub}} \leq 350°\text{C}$ when SM is different, the amorphous iridium oxide has been formed. While at $T_{\text{sub}} = 450°\text{C}$, the films were fully transformed to nanocrystalline single phase of IrO_2 at any concentration. Also, the increase in the intensity of the peaks with increasing the SM may be attributed to either grain growth or the increase in the degree of crystallinity or both. The variation in crystallite size was observed at different SM, because the concentration and mobility of ions were appropriate for crystal growing on the substrate. Also, it was mentioned to maximum value at higher SM that this is probably because the mobility and collision of ions are sufficient to recombine the crystal agglomerate. The behavior of electrical conductivity as a function of concentration was observed and the IrO_2 films may be possible transformation from semiconducting phase to metallic one. The values of ΔE and σ_o were found to be 0.21 eV and $1.68 \times 10^{-3}\,\Omega^{-1} \cdot \text{cm}^{-1}$, respectively.

References

[1] I. A. Ges, B. L. Ivanov, D. K. Schaffer, E. A. Lima, A. A. Werdich, and F. J. Baudenbacher, "Thin-film IrO_x pH microelectrode for microfluidic-based microsystems," *Biosensors and Bioelectronics*, vol. 21, no. 2, pp. 248–256, 2005.

[2] S. Sao, M. Wang, and M. Madou, "A pH electrode based on melt-oxidized iridium oxide," *Journal of the Electrochemical Society*, vol. 148, no. 44, pp. H29–H36, 2001.

[3] A. Karthigeyan, R. P. Gupta, K. Scharnagl, M. Burgmair, S. K. Sharma, and I. Eisele, "A room temperature HSGFET ammonia sensor based on iridium oxide thin film," *Sensors and Actuators B*, vol. 85, no. 1-2, pp. 145–153, 2002.

[4] A. E. Grumet, J. L. Wyatt, and J. F. Rizzo, "Multi-electrode stimulation and recording in the isolated retina," *Journal of Neuroscience Methods*, vol. 101, no. 1, pp. 31–42, 2000.

[5] T. J. Park, D. S. Jeong, C. S. Hwang, M. S. Park, and N. S. Kang, "Fabrication of ultrathin IrO_2 top electrode for improving thermal stability of metal-insulator-metal field emission cathodes," *Thin Solid Films*, vol. 471, no. 1-2, pp. 236–242, 2005.

[6] H. S. Lee, W. S. Um, K. T. Hwang, H. G. Shin, Y. B. Kim, and K. H. Auh, "Ferroelectric properties of $Pb(Zr,Ti)O_3$ thin films deposited on annealed IrO_2 and Ir bottom electrodes," *Journal of Vacuum Science and Technology A*, vol. 17, no. 5, pp. 2939–2943, 1999.

[7] S. Hackwood, G. Beni, M. A. Bösch, K. Kang, L. M. Schiavone, and J. L. Shay, "New process for optical information storage," *Physical Review B*, vol. 26, no. 12, pp. 7073–7075, 1982.

[8] S. F. Cogan, P. R. Troyk, J. Ehrlich, T. D. Plante, and D. E. Detlefsen, "Potential-biased, asymmetric waveforms for charge-injection with activated iridium oxide (AIROF) neural stimulation electrodes," *IEEE Transactions on Biomedical Engineering*, vol. 53, no. 2, pp. 327–332, 2006.

[9] A. Neubecker, T. Pompl, T. Doll, W. Hansch, and I. Eisele, "Ozone-enhanced molecular beam deposition of nickel oxide

(NiO) for sensor applications," *Thin Solid Films*, vol. 310, no. 1-2, pp. 19–23, 1997.

[10] P. S. Patil, R. K. Kawar, S. B. Sadale, A. I. Inamdar, and S. S. Mahajan, "Promotion of electrochromism in spray-deposited molybdenum oxide-doped iridium oxide thin films," *Solar Energy Materials and Solar Cells*, vol. 90, no. 11, pp. 1629–1639, 2006.

[11] C. Grangvist, *Handbook of Inorganic Electrochromic Materials*, Elsevier, Amsterdam, The Netherlands, 1995.

[12] S. S. Thanawala, R. J. Baird, D. G. Georgiev, and G. W. Auner, "Amorphous and crystalline IrO_2 thin films as potential stimulation electrode coatings," *Applied Surface Science*, vol. 254, no. 16, pp. 5164–5169, 2008.

[13] Y. Ritterhaus, T. Hur'yeva, M. Lisker, and E. P. Burte, "Iridium thin films deposited by liquid delivery MOCVD using Ir(EtCp)(1,5-COD) with toluene solvent," *Chemical Vapor Deposition*, vol. 13, no. 12, pp. 698–704, 2007.

[14] K. Nishio, Y. Watanabe, and T. Tsuchiya, "Preparation and properties of electrochromic iridium oxide thin film by sol-gel process," *Thin Solid Films*, vol. 350, no. 1, pp. 96–100, 1999.

[15] L. M. Zhang, Y. S. Gong, C. B. Wang, Q. Shen, and M. X. Xia, "Substrate temperature dependent morphology and resistivity of pulsed laser deposited iridium oxide thin films," *Thin Solid Films*, vol. 496, no. 2, pp. 371–375, 2006.

[16] J. Kristóf, T. Szilágyi, E. Horváth, A. De Battisti, R. L. Frost, and A. Rédey, "Investigation of IrO_2/Ta_2O_5 thin film evolution," *Thermochimica Acta*, vol. 413, no. 1-2, pp. 93–99, 2004.

[17] P. S. Patil, P. S. Chigare, S. B. Sadale, T. Seth, D. P. Amalnerkar, and R. K. Kawar, "Thickness-dependent properties of sprayed iridium oxide thin films," *Materials Chemistry and Physics*, vol. 80, no. 3, pp. 667–675, 2003.

[18] S. A. Mahmoud, A. A. Akl, H. Kamal, and K. Abdel-Hady, "Opto-structural, electrical and electrochromic properties of crystalline nickel oxide thin films prepared by spray pyrolysis," *Physica B*, vol. 311, no. 3-4, pp. 366–375, 2002.

[19] A. A. Akl, "Optical properties of crystalline and non-crystalline iron oxide thin films deposited by spray pyrolysis," *Applied Surface Science*, vol. 233, no. 1–4, pp. 307–319, 2004.

[20] B. P. Asthana and W. Kiefer, "Deconvolution of the Lorentzian linewidth and determination of fraction Lorentzian character from the observed profile of a Raman line by a comparison technique," *Applied Spectroscopy*, vol. 36, no. 3, pp. 250–257, 1982.

[21] S. A. Mahmoud, "Characterization of thorium dioxide thin films prepared by the spray pyrolysis technique," *Solid State Sciences*, vol. 4, no. 2, pp. 221–228, 2002.

[22] L. J. Van der Pauw, "A method of measuring specific resistivity and Hall effect of discs of arbitrary shape," *Philips Research Reports*, vol. 13, pp. 1–9, 1958.

[23] A. A. Ramadan, R. D. Gould, and A. Ashour, "On the Van der Pauw method of resistivity measurements," *Thin Solid Films*, vol. 239, no. 2, pp. 272–275, 1994.

[24] M. A. El Khakani and M. Chaker, "Reactive pulsed laser deposition of iridium oxide thin films," *Thin Solid Films*, vol. 335, no. 1-2, pp. 6–12, 1998.

[25] N. Bestaoui, E. Prouzet, P. Deniard, and R. Brec, "Structural and analytical characterization of an iridium oxide thin layer," *Thin Solid Films*, vol. 235, no. 1-2, pp. 35–42, 1993.

[26] R. K. Kawar, P. S. Chigare, and P. S. Patil, "Substrate temperature dependent structural, optical and electrical properties of spray deposited iridium oxide thin films," *Applied Surface Science*, vol. 206, no. 1–4, pp. 90–101, 2003.

[27] T. Sameshima, K. Saitoh, N. Aoyama, S. Higashi, M. Kondo, and A. Matsuda, "Electrical properties of pulsed laser crystallized silicon films," *Japanese Journal of Applied Physics*, vol. 38, no. 4, pp. 1892–1897, 1999.

[28] S. A. Mahmoud, A. A. Akl, and S. M. Al-Shomar, "Effect of some preparative parameters on optical properties of spray deposited iridium oxide thin films," *Physica B*, vol. 404, no. 16, pp. 2151–2158, 2009.

[29] C. Das and S. Ray, "Onset of microcrystallinity in silicon thin films," *Thin Solid Films*, vol. 403-404, pp. 81–85, 2002.

[30] R. Sanjinés, A. Aruchamy, and F. Lévy, "Metal-non metal transition in electrochromic sputtered iridium oxide films," *Solid State Communications*, vol. 64, no. 5, pp. 645–650, 1987.

[31] C. Battaglin, A. Carnera, P. Mazzoldi, et al., "Application of rutherford backscattering to non-destructive analysis of insoluble oxide electrodes," *Journal of Electroanalytical Chemistry*, vol. 135, no. 2, pp. 313–319, 1982.

[32] S. Gottesfeld, "Faradaic processes at the IR/IR oxide electrode," *Journal of the Electrochemical Society*, vol. 127, no. 9, pp. 1922–1925, 1980.